

Persistent single-photon production by tunable on-chip micromaser with a superconducting quantum circuit

J. Q. You,^{1,2} Yu-xi Liu,¹ C. P. Sun,^{1,3} and Franco Nori^{1,4}

¹Frontier Research System, The Institute of Physical and Chemical Research (RIKEN), Wako-shi 351-0198, Japan

²Department of Physics and Surface Physics Laboratory (National Key Laboratory), Fudan University, Shanghai 200433, China

³Institute of Theoretical Physics, Chinese Academy of Sciences, Beijing 100080, China

⁴Center for Theoretical Physics, Physics Department, Center for the Study of Complex Systems, University of Michigan, Ann Arbor, MI 48109-1040, USA

(Dated: May 24, 2019)

We propose a tunable on-chip micromaser using a superconducting quantum circuit (SQC). By taking advantage of externally controllable state transitions, a state population inversion can be achieved and preserved for the two working levels of the SQC and, when needed, the SQC can generate a single photon. We can regularly repeat these processes in each cycle when the previously generated photon in the cavity is decaying, so that a periodic sequence of single photons can be produced persistently. This provides a controllable way for implementing a persistent single-photon source on a microelectronic chip.

Superconducting quantum circuits can behave like natural atoms and are also promising candidates of qubits for scalable quantum computing [1]. Moreover, these circuits also show quantum optical effects and provide exciting opportunities for demonstrating quantum effects at macroscopic scales and for conducting atomic-physics experiments on a microelectronic chip (see, e.g., [1, 2, 3, 4, 5, 6, 7, 8]).

Because of its fundamental importance in quantum communications, single-photon sources are crucial in both quantum optics and quantum electronics [9]. Single-photon sources can be achieved using quantum-dot-based devices (see, e.g., [10]), but their frequencies are not in the microwave regime required for superconducting qubits. Recently, there have been efforts to generate single photons by coupling a superconducting qubit to a superconducting resonator [4, 5, 11]. However, because the photon damps in the resonator, the generated single photon can only persist for a very short time.

Here we show how to persistently produce steady microwave single photons by a *tunable* micromaser using a superconducting quantum circuit (SQC). The physical mechanism is as follows: The SQC acts like a *controllable* artificial atom (AA) and is placed in a quantum electrodynamic cavity. By taking advantage of the externally controllable state transitions, one can pump the AA to produce state population inversion for the two working levels. This population inversion is preserved by turning off the transition to the ground state, but when needed this transition can be switched on to generate a photon. Within the photon lifetime of the cavity, one can pump the superconducting AA to produce the state population inversion again for the next cycle of operations and then switch on the state transition when the photon generated in the previous cycle is decaying. By periodically repeating this cycle, one can generate single photons in a persistent way.

Steady-state photons can also be generated by a mi-

cromaser with natural atoms (see, e.g., [12]). However, in such a micromaser, there is a very small number of excited atoms among all atoms passing through the cavity and these excited atoms enter the cavity at *random* times. This will produce large fluctuations for the photon field of the cavity. For instance, an excited atom can enter the cavity long before or after the previously generated single photon decays. To overcome this problem, a state population inversion is prepared for the superconducting AA in each cycle and all the cycles are repeated periodically. Also, the cavity can be realized using an on-chip superconducting resonator (e.g., the transmission line resonator [4]), so that both the SQC and the resonator can be fabricated on a chip. This might be helpful for transferring quantum information between superconducting qubits in future applications. Moreover, in contrast with the fixed difference between the two working energy levels in a natural atom, the level difference for the superconducting AA is tunable, providing flexibility for producing a single-photon source over a wider frequency region.

Superconducting artificial atom.—We consider a SQC used for the so-called flux qubit [13]. This quantum circuit can behave like an AA. As shown in Fig. 1(a), in addition to two identical Josephson junctions, a symmetric SQUID is also placed in the loop pierced by an external magnetic flux Φ_e . This SQUID increases the external controllability of the quantum circuit by providing a tunable effective coupling energy: αE_J with $\alpha = 2\gamma \cos(\pi\Phi_s/\Phi_0)$, where Φ_0 is the flux quantum. The Hamiltonian of the system is

$$H = \frac{P_p^2}{2M_p} + \frac{P_m^2}{2M_m} + U(\varphi_p, \varphi_m), \quad (1)$$

with $P_i = -i\hbar\partial/\partial\varphi_i$ ($i = p, m$), $M_p = 2C_J(\Phi_0/2\pi)^2$, and $M_m = M_p(1 + 4\gamma)$. The potential $U(\varphi_p, \varphi_m)$ is $U(\varphi_p, \varphi_m) = 2E_J(1 - \cos\varphi_p \cos\varphi_m) + 2\gamma E_J[1 - \cos(\pi f_s) \cos(2\pi f + 2\varphi_m)]$, where $\varphi_p = (\varphi_1 + \varphi_2)/2$ and

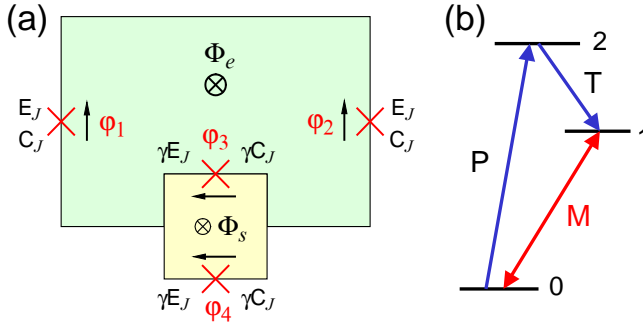


FIG. 1: (Color online) (a) Schematic diagram of the superconducting quantum circuit. A symmetric SQUID and two identical Josephson junctions with coupling energy E_J and capacitance C_J are placed in a superconducting loop pierced by an externally applied magnetic flux (green) Φ_e . The two Josephson junctions in the symmetric SQUID have coupling energy γE_J and capacitance γC_J , and the applied flux (yellow) threading through the SQUID loop is Φ_s . Here we choose $\gamma = 0.5$ and $E_J/E_c = 100$, with $E_c = e^2/2C_J$ being the single-particle charging energy of the junction. (b) Transition diagram of three energy levels used for a tunable micromaser where the state transitions are externally controlled.

$\varphi_m = (\varphi_1 - \varphi_2)/2$. The reduced fluxes f_s and f are given by $f_s = \Phi_s/\Phi_0$ and $f = \Phi_e/\Phi_0 + f_s/2$.

To make a transition between two energy levels E_i and E_j of the superconducting AA, a microwave field $\Phi_w(t) = \Phi_w^{(0)} \cos(\omega_{ij}t + \theta)$ is applied through the larger superconducting loop of the quantum circuit. For a weak microwave field, the time-dependent perturbation Hamiltonian is $H'(t) = -I\Phi_w(t)$; where $I = -2\gamma I_c \cos(\pi f_s) \sin(2\pi f + 2\varphi_m)$ is the circulating supercurrent in the loop without the applied microwave field, and the critical current of the junction is defined as $I_c = 2\pi E_J/\Phi_0$. The transition matrix element between states $|E_i\rangle$ and $|E_j\rangle$ is $t_{ij} = \langle E_i | I \Phi_w^{(0)} | E_j \rangle$.

Figures 2(a)-2(c) display the dependence of the energy levels on the reduced flux f for three different values of f_s . For a symmetric SQUID with $\gamma = 0.5$, these values of f_s give rise to an effective Josephson coupling energy αE_J with $\alpha = 1, 0.77$, and 0.66 , respectively. At $f_s = 0$, the third and fourth energy levels become degenerate and other adjoining levels touch at the crossing points. When f_s increases, this state degeneracy is removed and gaps develop at the crossing points, more pronounced for higher levels. In Figs. 2(d)-2(e), we show the moduli of the transition matrix elements $|t_{ij}|$ for the lowest three levels. At $f_s = 0$, the transition matrix elements t_{01} , t_{02} and t_{12} become zero in a wider region around $f = 0.5$. This means that the corresponding state transitions are forbidden. With f_s increasing, these state transitions become allowed, but the modulus of each transition matrix element increases in a different manner. In contrast, $|t_{01}|$ for the state transition between the two lowest levels E_0 and E_1 increases slowly. Below we will explore

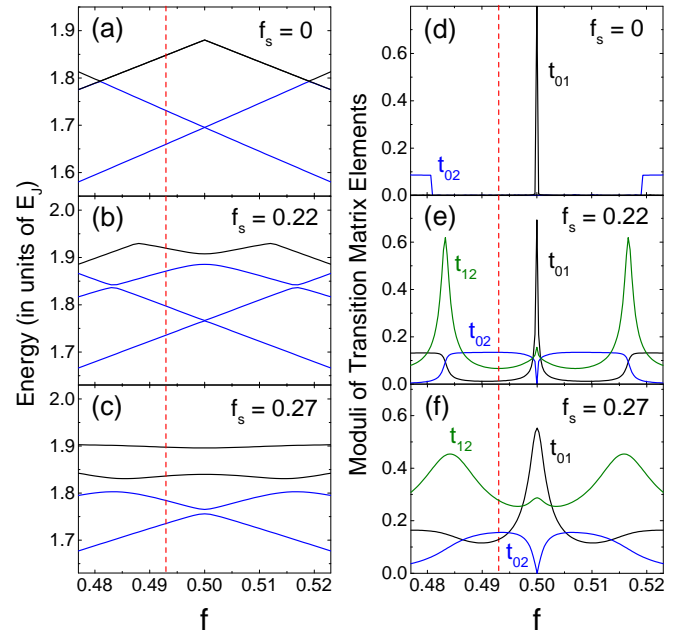


FIG. 2: (Color online) (a)-(c) Energy levels of the superconducting artificial atom versus the reduced magnetic flux $f = \Phi_e/\Phi_0 + f_s/2$ for $f_s (\equiv \Phi_s/\Phi_0) = 0, 0.22$, and 0.27 , where only the lowest four energy levels (E_i , $i = 0$ to 3) are shown. (d)-(f) Moduli of the transition matrix elements $|t_{ij}|$ (in units of $I_c \Phi_w^{(0)}$) versus the reduced flux f for $f_s = 0, 0.22$, and 0.27 . Two vertical (red) dashed lines are plotted at $f = 0.493$ as a guide to the eye.

these novel properties to implement a micromaser using a quantum circuit on a chip.

Fast adiabatic quantum-state control and state population inversion.—The state evolution of the superconducting AA depends on the external parameters. For two given quantum states $|E_i\rangle$ and $|E_j\rangle$, to have the evolution adiabatic, the nonadiabatic coupling $\langle E_i | \frac{d}{dt} | E_j \rangle$ and the energy difference $E_i - E_j$ should satisfy the condition [7]: $|\hbar \langle E_i | \frac{d}{dt} | E_j \rangle / (E_i - E_j)| \ll 1$. Here we change f_s but keep the reduced flux f unchanged. The adiabatic condition can be rewritten as $K_{ij} |df_s/dt| \ll 1$, where

$$K_{ij} = \left| \frac{\hbar \langle E_i | (\partial H / \partial f_s) | E_j \rangle}{(E_i - E_j)^2} \right|. \quad (2)$$

Figure 3 shows the quantities K_{01} and K_{12} as a function of the reduced flux f for different values of f_s . For instance, in the vicinity of $f = 0.493$ (vertical dashed lines in Fig. 2), $K_{01} \sim 0.2$ for $f_s = 0.27$ [see Fig. 3(a)]. We can have $K_{01} (df_s/dt) \sim 0.02 \ll 1$ with $df_s/dt = 0.1 \text{ ns}^{-1}$, corresponding to a speed of changing Φ_s , $d\Phi_s/dt \sim 0.1\Phi_0$ per ns. When $f_s = 0.22$, $K_{01} (df_s/dt) \sim 0.02$ for $df_s/dt = 2 \text{ ns}^{-1}$, and $d\Phi_s/dt$ can be much faster, to have the adiabatic condition satisfied by decreasing f_s . Also, around $f = 0.493$, $K_{12} \sim 0.4$ for $f_s = 0.27$ [see Fig. 3(b)]. When $df_s/dt = 0.1 \text{ ns}^{-1}$, $K_{12} (df_s/dt) \sim 0.04 \ll 1$, implying that the adiabatic condition is satisfied. For a smaller

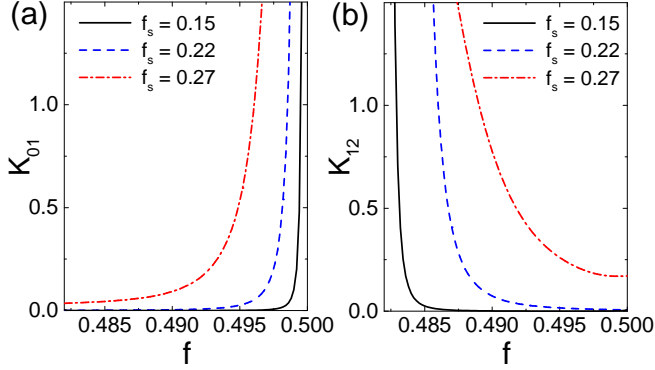


FIG. 3: (Color online) The quantities (a) K_{01} and (b) K_{12} for the adiabatic condition versus the reduced flux f for $f_s = 0.15, 0.22$, and 0.27 , respectively. Here we use $E_J = 400$ GHz.

f_s , K_{12} decreases significantly and a much higher $d\Phi_s/dt$ can be used. This important property reveals that, at $f \sim 0.493$, one can *adiabatically* manipulate the quantum states $|E_0\rangle$ and $|E_1\rangle$ of the superconducting AA by quickly changing f_s (e.g., $d\Phi_s/dt \gtrsim 0.1\Phi_0$ ns $^{-1}$) in the region of $0 \leq f_s \lesssim 0.27$.

Below we manipulate the superconducting AA around our example case $f = 0.493$ (the two vertical dashed lines in Fig. 2) by changing the flux Φ_s threading through the SQUID loop in three successive processes [see Fig. 1(b)]: (i) *Pumping process*: First, the quantum circuit works at $f_s = 0.22$. We constantly pump the superconducting AA with an appropriate microwave field to make the state transition $|E_0\rangle \rightarrow |E_2\rangle$ for a period of time. Simultaneously, another microwave field is also used to trigger the transition $|E_2\rangle \rightarrow |E_1\rangle$. For $f_s = 0.22$, $|t_{01}| \approx 0.01$, $|t_{12}| \approx 0.07$, and $|t_{02}| \approx 0.13$. Because $|t_{01}|$ is about one order of magnitude smaller than $|t_{12}|$ and $|t_{02}|$, a population inversion between the two lowest states $|E_0\rangle$ and $|E_1\rangle$ can be readily achieved. (ii) *Preserving the population inversion*: We decrease f_s to $f_s = 0$. Because $|t_{01}|$ now tends to zero, the transition $|E_1\rangle \rightarrow |E_0\rangle$ is forbidden and the state population inversion is preserved. (iii) *Switching-on process*: We increase f_s to $f_s = 0.27$ to turn on the transition $|E_1\rangle \rightarrow |E_0\rangle$ with an appreciable probability (i.e., $|t_{01}| \approx 0.13$, which is one order of magnitude larger than $|t_{01}| \approx 0.01$ at $f_s = 0.22$).

Micromaser and single-photon source.—Let us place the superconducting AA in a quantum cavity, with the energy difference $E_1 - E_0$ at $f = 0.493$ and $f_s = 0.27$ in resonance with the cavity mode. In the switching-on process, the superconducting AA acts as a two-level system and interacts with a single-mode quantized microwave field via Rabi oscillations, i.e., a coherent exchange of energy between them. The interaction Hamiltonian is given by $H' = -\hbar g(\sigma_+ a + \text{H.c.})$, where $g = |t_{01}|/2\hbar$, $\sigma_+ = |E_1\rangle\langle E_0|$, and a is the annihilation operator of photons of the cavity mode. We assume that the interaction between the cavity and the AA is in the strong-coupling

regime, where the period $1/2g$ of the single-photon Rabi oscillations is much shorter than both the relaxation time of the two-level system and the average lifetime of the photon in the cavity. After an interaction time τ , the quantum circuit turns to the pumping and population-inversion-preserving processes and it becomes ready for the next cycle of the three successive processes described above.

If the superconducting AA is switched on at the times t_i to interact with the photons in the cavity, the time evolution of the density matrix ρ of the cavity mode is governed by the map $\rho(t_i + \tau) = M(\tau)\rho(t_i)$, where the gain operator $M(\tau)$ is defined as $M(\tau)\rho = \text{Tr}_a[\exp(-iH'\tau/\hbar)\rho \otimes |E_1\rangle\langle E_1| \exp(iH'\tau/\hbar)]$, where Tr_a denotes the trace over the variables of the AA. Here we *regularly* switch on the superconducting AA by periodically repeating the cycle of the three successive processes. With the cavity losses included, the dynamics of the density matrix ρ is described by

$$\frac{d\rho}{dt} = r_a[M(\tau) - 1]\rho - \frac{1}{2}r_a(M - 1)^2\rho + L\rho. \quad (3)$$

In Eq. (3), r_a is the switching-on rate for the superconducting AA. The operator L describes the dissipation of the cavity photon due to a thermal bath: $L\rho = -\frac{1}{2}\kappa(n_{\text{th}} + 1)(a^\dagger a\rho + \rho a^\dagger a - 2a\rho a^\dagger) - \frac{1}{2}\kappa n_{\text{th}}(aa^\dagger\rho + \rho aa^\dagger - 2a^\dagger\rho a)$, where n_{th} is the average number of thermal photons in the cavity and κ is the photon damping rate.

At steady state, $d\rho/dt = 0$, which leads to a recursion relation for the steady photon number distribution $p_n = \langle n|\rho|n\rangle$ of the cavity mode:

$$p_{n+1} = \left[\frac{n_{\text{th}}}{n_{\text{th}} + 1} + \frac{2N_t S(n+1) + S^2(n+1)}{2(n_{\text{th}} + 1)(n+1)} \right] p_n - \frac{N_t S(n+1) S(n)}{2(n_{\text{th}} + 1)(n+1)} p_{n-1}, \quad (4)$$

where $n = 0, 1, 2, \dots$, $S(n) = \sin^2(g\tau\sqrt{n})$, $N_t = r_a/\kappa$ represents the number of cycles for switching on the superconducting AA during the photon lifetime of the cavity, and p_0 is determined by $\sum_{n=0}^{\infty} p_n = 1$. This is in sharp contrast with the recursion relation for the atomic micromaser, where all the excited atoms enter the cavity at random times [12]: $(n_{\text{th}} + 1)np_n = [n_{\text{th}}n + N_t S(n)]p_{n-1}$, where $N_t = \bar{r}_a/\kappa$, with \bar{r}_a being the *average* injection rate of the excited atoms.

In Fig. 4(a), we present the steady-state photon statistics for $N_t = 100$. The statistics reveals an appreciable difference between the micromaser with natural atoms and that with a superconducting AA. Moreover, we show the steady-state photon statistics for $N_t = 1$ [see Fig. 4(b)]. It is striking that the single-photon state has a probability at least one order of magnitude larger than multi-photon states. For an atomic micromaser, the excited atoms enter the cavity at random times and obey a Poissonian distribution. Because the number n_{ex}

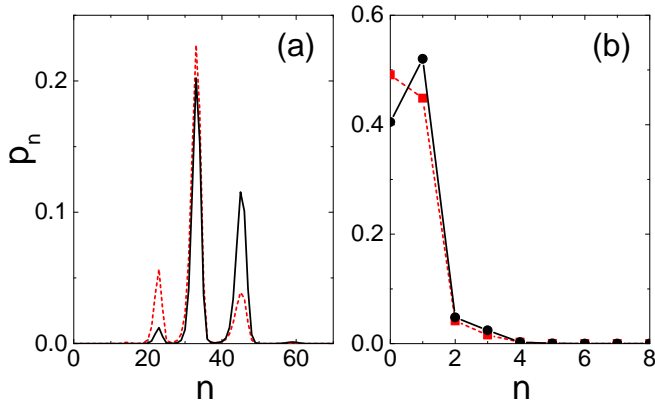


FIG. 4: (Color online) Steady-state photon statistics for $n_{\text{th}} = 0.1$, and (a) $N_t = 100$, $\tau_{\text{int}} (\equiv g\tau\sqrt{N_t}) = 10\pi$; (b) $N_t = 1$, $\tau_{\text{int}} = 1.4\pi$. These are results for a micromaser using either our quantum circuit (black solid lines) or natural atoms, e.g., rubidium (red dashed lines).

of the excited atoms has a larger variance, $\overline{\Delta n_{\text{ex}}^2} = \overline{n}_{\text{ex}}$, to the average number \overline{n}_{ex} , larger fluctuations are expected for the photon field in the cavity. In contrast, in the micromaser using a SQC, the AA can be *regularly* switched on to interact with the photons in the cavity and the photon-field fluctuations are greatly reduced because $\overline{\Delta n_{\text{ex}}^2} \sim 0$. Therefore, one can use the SQC micromaser to implement a *persistent* single-photon source with low-field fluctuations.

Experimentally accessible quantities.—Let us consider a quasi-two-dimensional (2D) cavity, so that both the SQC and the cavity can be fabricated on the same chip. Moreover, the SQC is placed at an antinode of the cavity mode and the magnetic flux threads perpendicularly through the SQC loop. The quantized magnetic flux inside the SQC loop can be written as $\Phi_w = \Phi_w^{(0)}(a + a^\dagger)$, with $\Phi_w^{(0)} = (\hbar\nu/\epsilon_0 c^2 Ah)^{1/2} S_q$, where ν , A , h , and S_q are the cavity frequency, the area of the quasi-2D cavity, the thickness of the cavity, and the area of the SQC loop, respectively. At $f = 0.493$ and $f_s = 0.27$, the numerical results in Fig. 2(c) give that $E_1 - E_0 \approx 0.05E_J$. When this level difference is in resonance with the cavity mode, the frequency of the cavity mode is $\nu = (E_1 - E_0)/h \approx 20$ GHz for a typical value of $E_J/h = 400$ GHz; the wavelength is $\lambda \approx 1.5$ cm. Here, as an example, we use $A \sim (1.5 \text{ cm})^2$ and $h \sim 1 \mu\text{m}$ for the quasi-2D cavity. Moreover, as shown in [14], the energy spectrum is nearly unchanged up to $\beta_L \equiv L/L_J \sim 0.1$, where the Josephson inductance is defined by $L_J = \Phi_0/2\pi I_c$. This gives a loop inductance $L \approx 40$ pH and the diameter of the loop is about $32 \mu\text{m}$. Then, we have $\Phi_w^{(0)}/\Phi_0 \approx 1.1 \times 10^{-4}$.

Also, at $f = 0.493$ and $f_s = 0.27$, the numerical results in Fig. 2(f) give that $|t_{01}| = 0.13I_c\Phi_w^{(0)}$. Using the

values given above, we obtain $g = |t_{01}|/2\hbar \approx 109$ MHz. For $N_t = 1$ and $g\tau\sqrt{N_t} = 1.4\pi$ [cf. Fig. 4(b)], the corresponding interaction time τ for the AA to couple with the cavity mode in each cycle of operations is $\tau \approx 40$ ns. This value of τ is experimentally feasible because it is much shorter than the relaxation time T_1 of the flux qubit (e.g., $T_1 \sim 1 \mu\text{s}$ in [2]) and also can easily be much shorter than the photon lifetime of an experimentally accessible high-Q superconducting cavity.

In conclusion, we have proposed a tunable on-chip micromaser using a SQC. By taking advantage of the externally controllable transitions between states, we can both produce and preserve a state population inversion for the two working levels of the SQC. When the previously generated photon in the cavity is decaying, the SQC can generate a new single photon. These processes can be regularly repeated to produce single photons in a persistent manner. This scheme provides a controllable way for implementing a persistent single-photon source on a microelectronic chip.

This work was supported in part by the NSA and ARDA under AFOSR contract No. F49620-02-1-0334, and by the NSF grant No. EIA-0130383. J.Q.Y. was also supported by the NSFC grant Nos. 10474013 and 10534060. C.P.S. was partially supported by the NSFC and the NFRPC.

- [1] J.Q. You and F. Nori, Phys. Today **58**(11), 42 (2005), and references therein.
- [2] I. Chiorescu *et al.*, Science **299**, 1869 (2003).
- [3] J.Q. You and F. Nori, Phys. Rev. B **68**, 064509 (2003); C.P. Yang, S.I. Chu, and S. Han, Phys. Rev. A **67**, 042311 (2003); A. Blais *et al.*, Phys. Rev. A **69**, 062320 (2004).
- [4] A. Wallraff *et al.*, Nature (London) **431**, 162 (2004).
- [5] Y.X. Liu, L.F. Wei, and F. Nori, Europhys. Lett. **67**, 941 (2004); Phys. Rev. A **71**, 063820 (2005).
- [6] A.M. Zagorskin, M. Grajcar, and A.N. Omelyanchouk, Phys. Rev. A **70**, 060301(R) (2004).
- [7] Y.X. Liu *et al.*, Phys. Rev. Lett. **95**, 087001 (2005).
- [8] P. Zhang, Y.D. Wang, and C.P. Sun, Phys. Rev. Lett. **95**, 097204 (2005); E.J. Pritchett and M.R. Geller, Phys. Rev. A **72**, 010301(R) (2005).
- [9] M. Oxborrow and A.G. Sinclair, Contemp. Phys. **46**, 173 (2005).
- [10] J. Kim *et al.*, Nature **397**, 500 (1999); P. Michler *et al.*, Science **290**, 2282 (2000); Z.L. Yuan *et al.*, *ibid.* **295**, 102 (2002).
- [11] M. Mariantoni *et al.*, cond-mat/0509737.
- [12] M.O. Scully and M. S. Zubairy, *Quantum Optics* (Cambridge University Press, Cambridge, 1997), Chapt. 13.
- [13] T.P. Orlando *et al.*, Phys. Rev. B **60**, 15398 (1999).
- [14] J.Q. You, Y. Nakamura, and F. Nori, Phys. Rev. B **71**, 024532 (2005).